CrystEngComm

Single crystalline Ge thin film growth on c-plane sapphire substrates by molecular beam epitaxy (MBE)

Journal:	*CrystEngComm*
Manuscript ID	CE-ART-12-2021-001715.R1
Article Type:	Paper
Date Submitted by the Author:	10-Apr-2022

Complete List of Authors:	Wangila, Emmanuel; University of Arkansas Fayetteville, Program of Materials Science and Engineering and Electrical Engineering, University of Arkansas, Fayetteville, Arkansas 72701, USA Saha, Samir; University of Arkansas Fayetteville, Physics Kumar, Rahul; Birla Institute of Technology and Science - Pilani Campus Kuchuk, Andrian; University of Arkansas Fayetteville Institute for Nanoscience and Engineering, Gunder, Calbi; University of Arkansas Fayetteville Amoah, Sylvester ; University of Arkansas Fayetteville Khiangte, Krsita; Indian Institute of Technology Bombay Chen, Zhong ; University of Arkansas Fayetteville Yu, Fisher; University of Arkansas, Arkansas Institute for Nanoscale Materials Science and Engineering Salamo, Gregory; University of Arkansas, Physics

Single crystalline Ge thin film growth on c-plane sapphire substrates by molecular beam epitaxy (MBE)

Emmanuel Wangila[1], Samir K. Saha[*1,4], Rahul Kumar[3,a], Andrian Kuchuk[3], Calbi Gunder[1], Sylvester Amoah[4], Krista R. Khiangte[3,b], Zhong Chen[4], Shui-Qing Yu[3,4], Gregory J. Salamo[2,3]

[1] *Program of Materials Science and Engineering, University of Arkansas, Fayetteville, Arkansas 72701, USA*

[2] *Department of Physics, University of Arkansas, Fayetteville, Arkansas 72701, USA*

[3] *Institute for Nanoscience and Engineering, University of Arkansas, Fayetteville, Arkansas 72701, USA*

[4] *Department of Electrical Engineering, University of Arkansas, Fayetteville, Arkansas 72701, USA*

Current address:

[a] *Department of Electrical and Electronics Engineering, Birla institute of Technology and Science, Pilani-333031, India*

[b] *Department of Physics, Banaras Hindu University, Varanasi, Uttar Pradesh 221005, India*

Abstract: Single crystalline Ge has been grown on c-plane sapphire substrates by molecular beam epitaxy. Direct growth of Ge on sapphire results in three-dimensional (3D) Ge islands, two growth directions, more than one primary domain, and twinned crystals. The introduction of a thin AlAs nucleation layer significantly improved the surface and material quality, which is evident from a smoother surface, single epitaxial orientation, sharper rocking curve, and a single domain. The AlAs nucleation layer thickness was also investigated, and a 10 nm AlAs layer resulted in the lowest surface roughness of 3.9 nm. We have been able to achieve a single primary domain and reduced twinning than previous works. A high-quality Ge buffer on sapphire has the potential as an effective platform for the subsequent growth of GeSn and SiGeSn for microwave photonics**.**

1. Introduction

Silicon photonics is one of the key emerging technologies addressing the growing internet traffic and the demand for secure and higher data rates. Current silicon photonic systems are made of discrete optical components on a silicon platform, which while effective, are sensitive to vibrations, temperature changes, and limited by interconnection speeds. As a result, research efforts are now focusing on integrating photonic devices, monolithically fabricated on a silicon photonic platform [1, 2]. The heart of this approach is the photonic chip, along with fiber arrays to couple light in and out of the chip. However, since silicon is an indirect bandgap material, the silicon chip is without an integrated laser source [3, 4]. As a result, the laser source, such as an InP based laser, must be separately bonded onto the chip [5, 6]. Consequently, this approach misses many of the advantages of a fully integrated monolithically fabricated photonic circuit. An approach that is now more aggressively pursued but at the research stage, is the growth of III-V quantum dots (QDs) directly onto silicon [7, 8]. Although an excellent approach, since QDs are formed by self-assembly, the resulting inhomogeneously broadened distribution in height leads to a large spread in wavelength and potentially a higher threshold. The approach must also deal with a thermal expansion mismatch and a low index contrast for waveguides on the silicon substrate [9]–[15].

An alternative approach investigated here is to use sapphire as a substrate in place of silicon. This approach brings together onto one platform two of the most important inventions of the 20th century: (1) the silicon integrated circuit and (2) the semiconductor laser. Together, they have the potential to enable faster data transfer rates than currently possible. The choice to investigate the sapphire platform is based on several advantages over current silicon technology, such as, (1) significantly greater immunity to the defects of space radiation [16], (2) high index contrast for efficient waveguides [17], (3) nearly perfect thermal expansion match to Group IV and III-V semiconductors for durability [18], and (4) the flexibility to support the monolithic fabrication of both laser and photonic integrated circuit on one platform, allowing higher function at reduced cost [19]. However, the approach must deal with a significant mismatch in lattice type and lattice constant.

In this paper, we report on the growth of Ge on a sapphire. The investigation is made as a first step to integrate group IV-based semiconductor alloys, such as GeSn and SiGeSn, on sapphire substrates. The outcome would make possible the fabrication of near to mid infrared optical

devices on a substrate ideal for microwave electronics. More specifically, we present results on the epitaxial growth of Ge thin (~50 nm) films on c-plane sapphire substrates using different growth temperatures and buffer layers to achieve high quality material. We have characterized these samples by both atomic force microscopy (AFM) and high-resolution X-ray diffraction (HRXRD), to observe the crystal morphology, quality, and structure.

2. Experiment

All samples were grown using a Riber-32 molecular beam epitaxy (MBE) growth system. The preparation for the sapphire substrate before the growth is discussed in our previous reports [16, 17], [19]. Consequently, all sapphire substrates, used in this work, possessed atomic step-terrace surface, consisting of one monolayer with 0.2-0.3 nm high steps and non-uniform terraces having widths of 200 nm to 300 nm. Prepared substrates are transferred to either (a) the group IV chamber for growth of Ge or (b) to the group III-V arsenic chamber for growth of an AlAs nucleation layer, before transfer to the IV chamber for growth of Ge. Previous work [20, 21] on the growth of Ge on sapphire did not explore the possibility of an AlAs buffer. The growth rate of Ge and AlAs were 0.16 ML/s and 0.2 ML/s, respectively. In-situ reflection high energy electron diffraction (RHEED), with electrons accelerated at 20 keV at 1.5 A at a glancing angle of 1° to 2° to the substrate, was used to observe oscillations from homoepitaxial Ge and AlAs/GaAs samples to provide growth rate calibrations.

The intermittent contact mode of atomic force microscopy (AFM) (Bruker, model number 3000 dimension III) was also used to study the surface morphology. A sharp Si tip with a tip radius of about 10 nm, along with optimized feedback and force parameters, were used for the AFM imaging. The PANalytical X'pert MRD diffractometer, equipped with a CuKα1 source of radiation (λ=0.15406 nm), multilayer focusing mirror, four bounce Ge (220) monochromator, and a Pixel detector, were used to examine the crystal quality.

3. Growth and discussion

(a) Direct growth of Ge on sapphire

At the start of our investigation, Ge was grown directly on prepared sapphire substrates at four different growth temperatures (T_G): 400°C, 500°C, 600°C and 800°C. For each sample, the nominal thickness and growth rate were kept at 50 nm and 0.16 ML/s, respectively. As shown by (5×5 μm^2) AFM images (Fig. 1), the high lattice mismatch and interface energy between Ge and the sapphire substrate (Ge-O (657.5±4.6 kJ/mol, Ge-Ge (264.4±6.8 kJ/mol)) promoted 3D growth. An estimate of the average height of the 3D islands, island density, average roughness, and deposited material amount, were determined from the AFM images for all growth temperatures and are listed in Table 1. With increasing T_G, the island size increased due to ripening, until a temperature of T_G = 800°C, at which we observe a clear decrease in island size. This behavior was also reported by Godbey *et al* [20, 21]. The decrease in island size was first unexpected since at higher T_G normally enhances adatom diffusion, normally resulting in larger island size and lower density [16]. However, the smaller island size at T_G = 800°C can be explained by considering the rate of ripening compared to the rate of Ge deposition and desorption. If at equilibrium the rate of ripening is lower than the desorption of adatoms, the Ge islands can maintain a small size and high density with the incident Ge flux. This possibility is consistent with the fact that the effective thickness of the sample grown at T_G = 800°C is significantly less than their counterparts at T_G = 400°C, 500°C, 600°C under the same incident Ge flux growths.

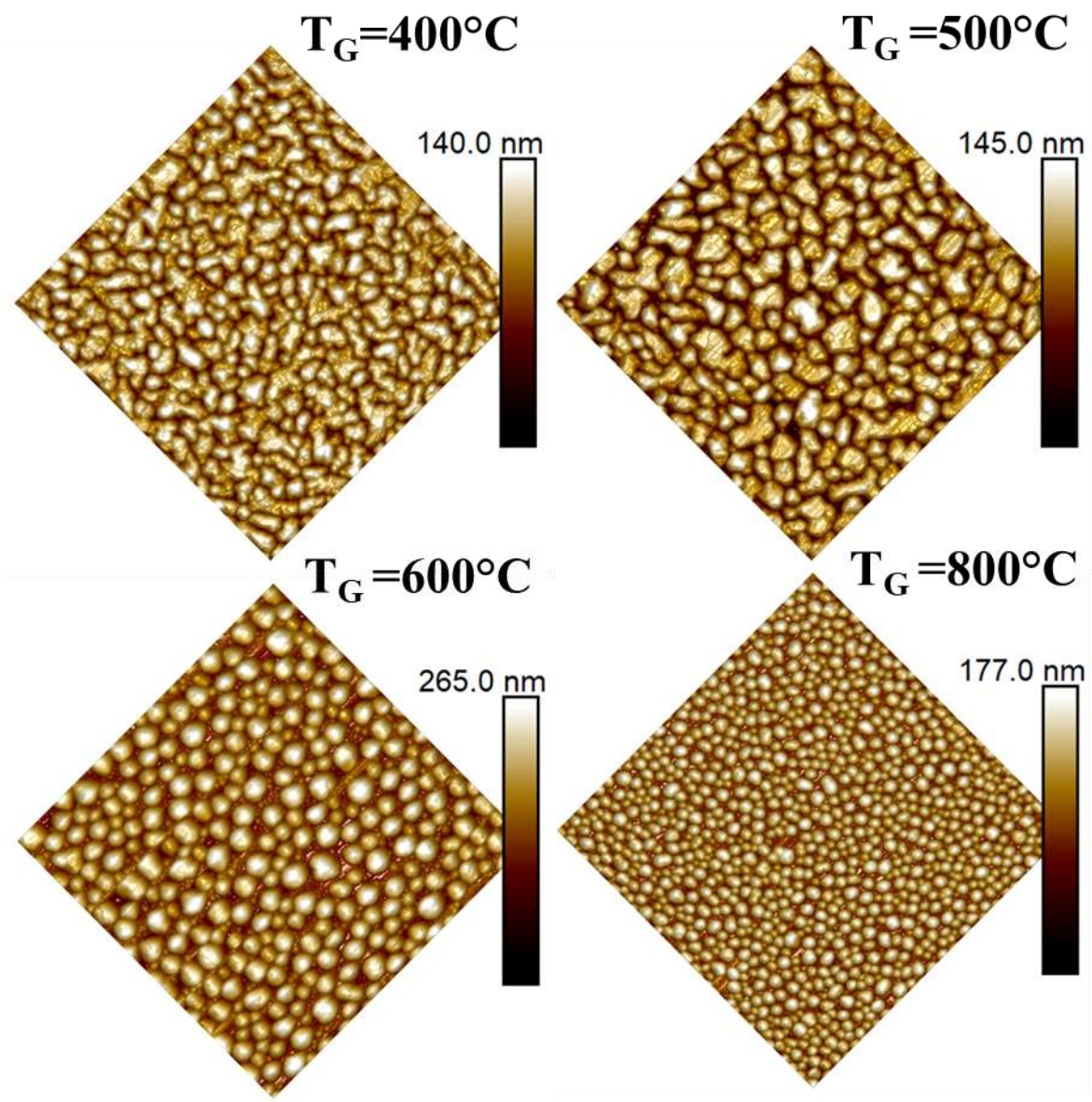

Figure 1: Surface morphology are shown for samples grown at different growth temperatures: (a) T_G = 400°C, (b) T_G = 500°C, (c) T_G = 600°C, and (d) T_G = 800°C.

Table 1: Average surface characteristics for each Ge on sapphire at different T_G

T_G (°C)	Average height (nm)	Density (cm^{-2})	Surface roughness (nm)	Material Deposited (nm)
400	44±2	1.0E9	14.2	50±5
500	67±4	1.6E9	17.2	51±4
600	69±4	5.8E9	33.0	55±2
800	69±4	1.0E9	16.8	35±5

XRD ω-2θ scans were performed to determine and compare crystal quality for each of these samples. A sharp peak at $2\theta \approx 41.7°$ is due to a bulk (00.6) reflection from the sapphire substrate. As shown in Fig. 2(a), two different orientations, (111) and (220), are observed except at T_G = 600°C for which only a (111) reflection is observed for the sample grown at T_G = 600°C indicating that there exists a small growth window for single crystal growth.

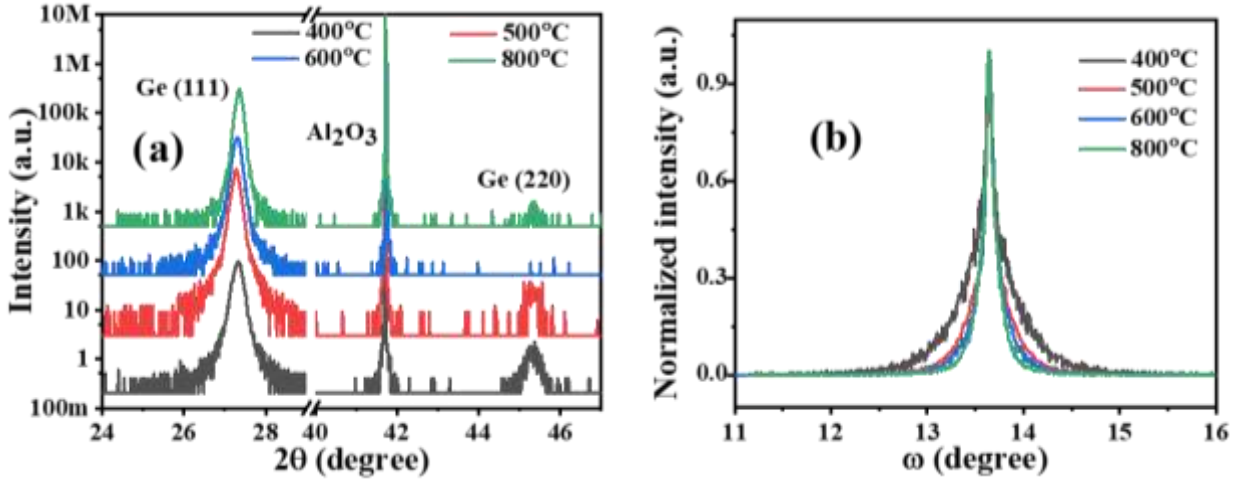

Figure 2: (a) XRD ω-2θ scan of Ge/sapphire system at different temperatures; (b) normalized ω scan for the crystal quality determination.

Likewise, we compared normalized rocking curve (RC) measurements for these samples in Fig. 2(b). The full width half maximum (FWHM) (Table 2) is observed to decrease with increased growth temperature indicating that the crystal quality improves at higher growth temperatures [21]. The lowest FWHM value is also observed for the sample grown at 600°C which is consistent with the ω-2θ scan measurement for which we have observed only Ge (111) oriented crystal growth.

Table 2: Full width half maximum at different T_G

T_G (°C)	FWHM (arc sec)
400	577
500	426
600	363
800	421

Asymmetric Ge (220) and sapphire (10.4) phi scans were also performed to further investigate the crystal quality of the grown epilayers. At T_G = 400°C and 500°C, 18 peaks are observed and among them 6 peaks are in pairs, as shown in Fig. 3(a). Between two pairs of peaks, a much smaller peak is observed. At T_G = 500°C, the smaller peaks are indicated by red arrows. The pairs are separated by approximately 7°, 10°, and 8° at 400°, 500°, and 800°C, respectively and at 600°C the pairs of peaks are nearly merged, and the small peaks vanish. This is again consistent with a window for growth at 600°C. That is, twin-free Ge (111) should give three (220) peaks separated by120° in the phi-scan [22]. Since at T_G = 400°C and 500°C, 18 peaks are observed, this indicates that there are three different growth domains which we indicated by A, B and C and are rotated from each other. Each of the three domains have the expected three family members and three twins which are separated by 120° and 60° respectively. At T_G = 600°C and 800°C, domain C has vanished. The phi scan of sapphire (10.4) is also shown by long violet dotted lines. Three lines indicate the trigonal space symmetry of c-plane sapphire which make ±4°and 30° with the Ge three primary domains.

Figure 3(b) shows the X-ray pole figure measurement of the sample grown at 400°C as an example. The measurement is performed at $\chi \sim 35 \pm 0.5°$. There are six weak spots observed for in-plane φ rotation, but they are also in pairs and marked by 1, 2 and 3. Therefore, three elongated weak spots are observed and separated by 120°. A similar pattern is also observed for the strong spots which are 60° in-plane apart from the weak spots. Between the weaker and strong spots, a small spot is observed, and it is marked by a red circle. There are six small spots 0-360° azimuthally separated by 60°. Therefore, the total 18 spots are observed in the pole figure

measurement at □~35 ± 0.5° which is consistent with φ measurements of Ge/sapphire system. The specific orientation of the A, B, and C domains are shown in Fig. 3(b).

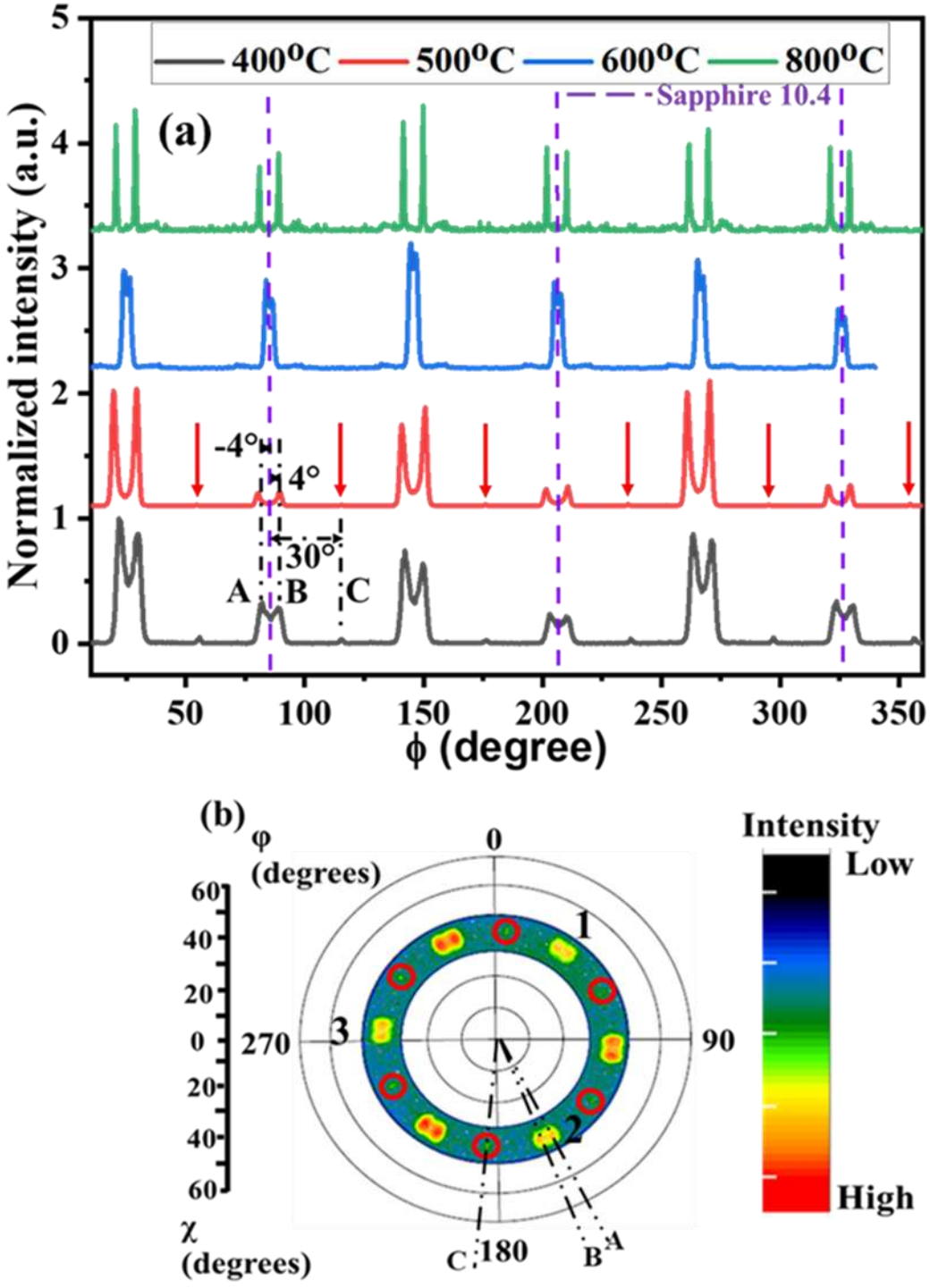

Figure 3 : (a) Phi scan for the in -plane orientation of Ge (220) crystal plane on sapphire at different temperatures. A, B and C indicates primary domain. (b) X-ray pole figure measurement of the sample grown at 400°C.

Consequently, the structure and orientation of each domain is observed in the phi-scans (Fig. 3 (a)) for these samples, relative to sapphire, and are depicted in Fig. 4. At 400℃ the primary domains A, B, and C are prominent, where domain C gradually decreases as the temperature increases and only two primary domains are left at 600°C and 800°C in the same primary domains position. Thus, choosing a sample grown at 400℃ is sufficient to show the orientation of the primary domains and sapphire substrates. Specifically, the in-plane relationship between sapphire (10.4) and three domains of Ge (220) are shown in Fig. 4. Hexagons shown by the broken lines represent the surface unit cell of Ge (111) whereas hexagons shown by the solid black lines represent the surface unit cell of c-plane sapphire. This suggests that there are two possible ways for the formation of three domains. First, it is possible that early in the growth of Ge on sapphire, instead of three different domains, only two domains existed. For these two domains, [110] direction of Ge is aligned with either the $[\bar{1}0.0]$ or $[\bar{1}2.0]$ (30° rotated than $[\bar{1}0.0]$) direction of sapphire. As a second possibility, as the coverage of Ge increases, the strain also increases, and the Ge domain align $[\bar{1}0.0]$ direction splits into two domains which makes ±4° along $[\bar{1}0.0]$ direction to reduce the strain energy. Similar observations have been reported in the case of GaAs on r-plane sapphire growth [16].

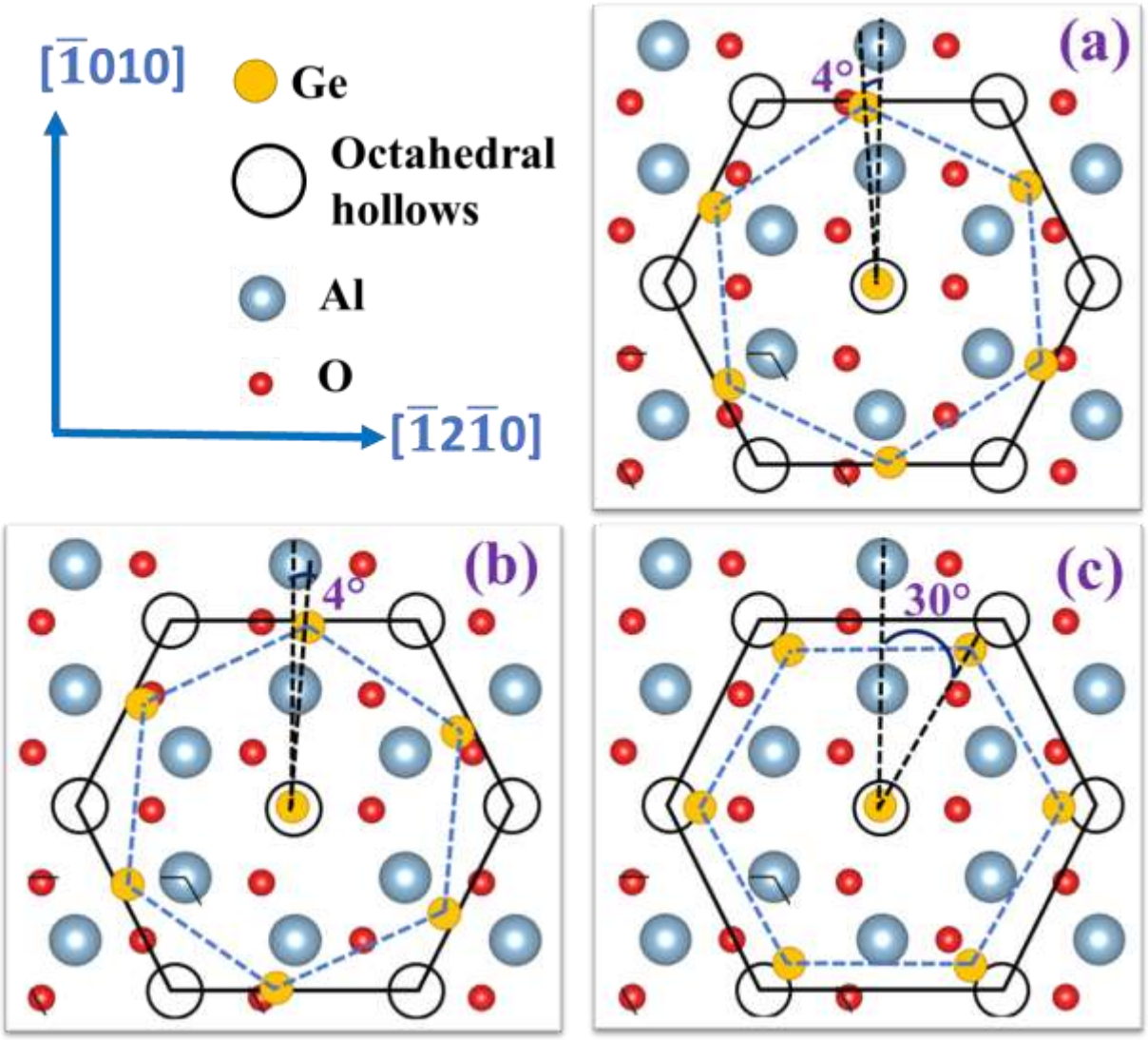

Figure 4: In plane alignment of Ge on c-plane sapphire for primary domain (a) A, (b) B, and (c) C. Dotted hexagons show the Ge (111) plane whereas hexagons surrounded by solid lines show the surface unit cell of c-plane sapphire, angles in the drawing show the angle between [1$\bar{1}$0] of Ge (in-plane direction of Ge (111)) and [$\bar{1}$0.0] of sapphire (in-plane direction of c-plane sapphire). Atomic distances are to the scale with small error.

(b) Seeded growth of Ge on AlAs on sapphire

For the direct growth of Ge on sapphire, we have observed 3D growth and different domains and twining. Even for the sample grown at 600°C in which we have observed only the (111) reflection in the XRD ω-2θ scan, the quality of the crystal is still characterized by 3D growth and different domains. Apparently, the stronger Ge-O bond (657 kJ/mol), when compared to Al-O (501 kJ/mol), is insufficient to overcome the mismatch in lattice constant. To overcome these limitations, we investigated the use of a thin nucleation layer (NL) of AlAs on the sapphire before the growth of Ge. AlAs as a NL utilizes both of its elements to bond with sapphire: Al from AlAs bonds to O while As bonds to Al enabling it to wet the sapphire substrate [17]. Moreover, AlAs has better lattice match with Ge making it more suitable as a NL for Ge epitaxy. Our approach was to examine the effect of a thin, 10 nm thick, buffer of AlAs grown at 700°C in the group III-V chamber which is UHV connected to the group IV MBE chamber. The growth details of AlAs on sapphire are described elsewhere [16, 17]. After growth of the AlAs thin nucleation layer, the AlAs/sapphire substrate was then transferred to group IV chamber through high vacuum transferred lines and subsequent growth of Ge (~50 nm) at temperatures between 250°C and 700°C. Fig. 5 shows the (2×2 μm^2) AFM images of the samples. The average island height, lateral size of the terraces, surface roughness, and amount of deposited material at different temperatures are listed in Table 3.

The results show that the average island height, lateral size of the terraces and surface roughness, all increased with temperature. For example, the average islands height, lateral size, and surface roughness, are 7 nm, 45 nm and 1.95 nm respectively at 250°C. With increasing temperature, coalescence between islands, increased the island height, lateral size, and surface roughness to 78 nm, 754 nm, and 32 nm respectively at 700°C. To gain a better perspective for these numbers, we fabricated a reference sample of 50 nm Ge (111) on a Ge (111) substrate at 400°C. The homoepitaxial Ge (111) grown sample surface roughness was 5.55 nm which was higher than what we achieved for the AlAs/sapphire substrate at 400°C. However, it is important to note that the morphology is different and consisted of valleys and plateaus at 400°C, 450°C and 700°C, with deeper valleys and flatter plateaus with increasing temperature.

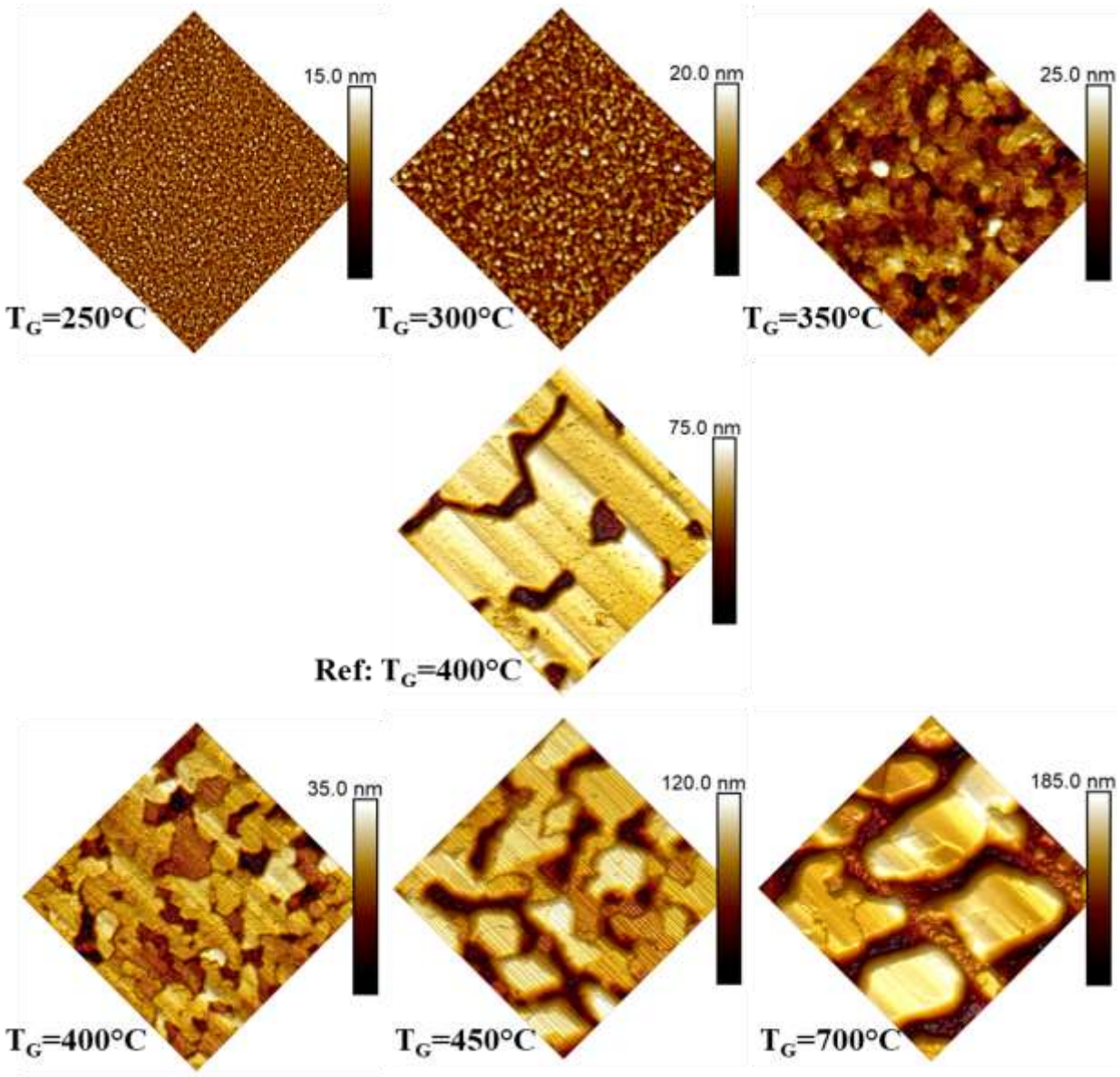

Figure 5: (2×2) AFM images for samples grown at different T_G (a) 250°C, (b) 300°C, (c) 350°C, (d) 400°C, (e) 450°C, and (f) 700°C.

Table 3: Surface roughness and thickness of material deposited at different T_G

Samples	Av. Height (nm)	Av. Lateral size (nm)	Surface Roughness (nm)	Material De-posited (nm)
X=250ºC	7	45	1.95	54±6
X=300ºC	7.2	96	2.46	57±2
X=350ºC	14	239	2.95	49±2
X=400ºC	22	325	3.9	54±6
Ref. - 400ºC	97	954	5.55	46±2
X=450ºC	59	545	16.4	51±4
X=700ºC	78	754	32	36±6

From the ω-2θ scan (Fig. 6(a)), we can see that the presence of the NL layer suppresses (220) formation at all growth temperatures. This implies that sample grown after the introduction of NL, is single crystalline. A small peak is also observed to the right side of Ge (111) reflection, which is due to the AlAs nucleation layer. It is also interesting to note that fringes were observed for the sample with the NL. This means that introduction of the NL potentially yields smooth plateaus. This result is consistent with the AFM image analysis. For analysis of crystal quality, we made rocking curve (RC) measurements (Fig. 6(b)) for which the FWHM are listed in Table 4. Analysis of the FWHM of the RC indicates a trend toward decreasing width with increasing growth temperature. The FWHM using NL is relatively less compared to direct growth of Ge at any growth temperatures. On this basis, the NL results a higher quality Ge film on sapphire. However, the FWHM of the homoepitaxial Ge (111) grown sample was 57 arcsec and higher quality than Ge (111) on sapphire. To further check the crystal quality of the samples we have also performed phi-scan on these samples as shown in Fig. 6(c). Here, introduction of an AlAs NL reduces the number of rotational domains and only six peaks are observed for all samples as compared to the 18 peaks for Ge grown directly on sapphire. This indicates that the application of AlAs NL improves the crystal quality of the epilayers. Results show that the minimum twin volume and the overall best quality of Ge thin films on sapphire with an AlAs NL is observed at 700°C.

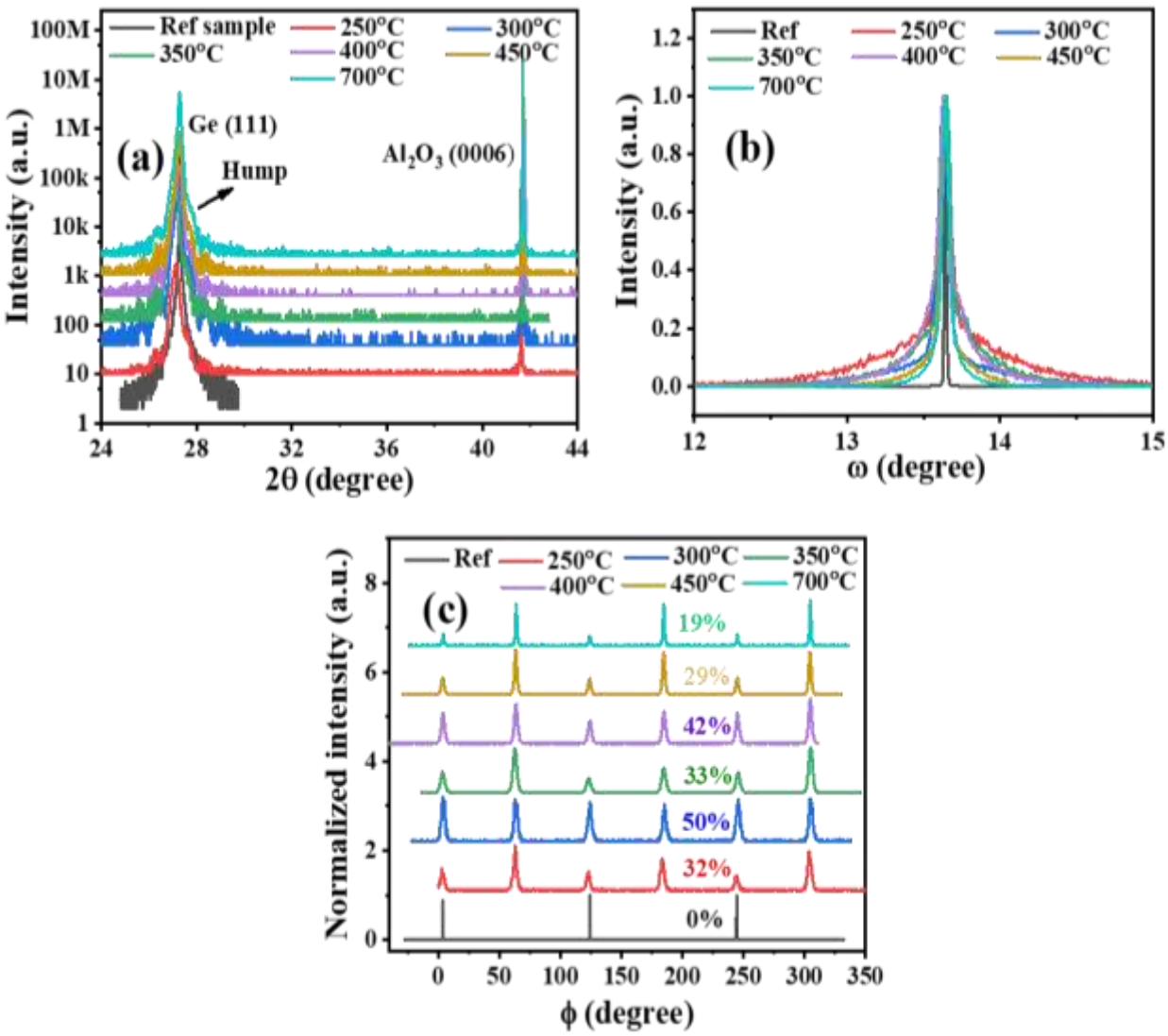

Figure 6: Out of plane measurements of Ge /AlAs/sapphire system, (b) RC measurements of Ge/AlAs/sapphire system, (c) in-plane measurements of Ge/AlAs/sapphire system.

Table 4: Full width half maximum of Ge/AlAs/sapphire at different T_G

Samples	FWHM (arc sec)
X=250ºC	368
X=300ºC	315
X=350ºC	315
X=400ºC	307
Ref. - 400ºC	58
X=450ºC	213
X=700ºC	213

(c) Effect of AlAs nucleation layer thickness:

Encouraged by these results, we have grown several samples in which we also varied the thickness of the AlAs NL layer. For example, growths with three different AlAs NL thicknesses, namely, 5, 10 and 15 nm, were grown. From analysis of the AFM surface images (Fig. 7), the rms surface roughness for the samples with AlAs NL thickness 5, 10, and 15 nm are 6.7, 3.9, and 3.98 nm, respectively. That is, the surface roughness relatively reduces from the sample whose AlAs NL is 5 nm to 10 nm with little change for 15 nm.

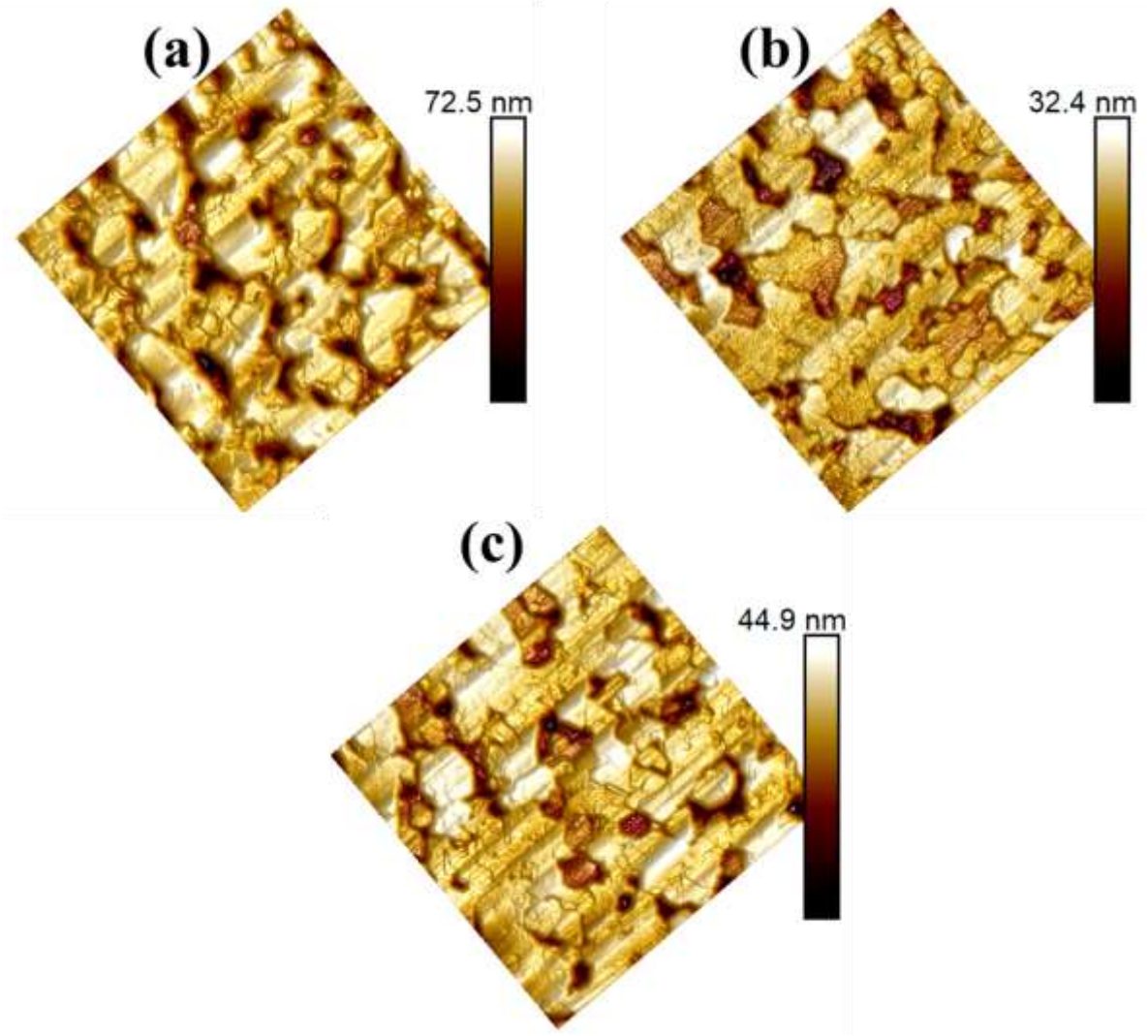

Figure 7: AFM image of the sample with AlAs NL thickness (a) 5 nm, (b) 10 nm and (c) 15 nm.

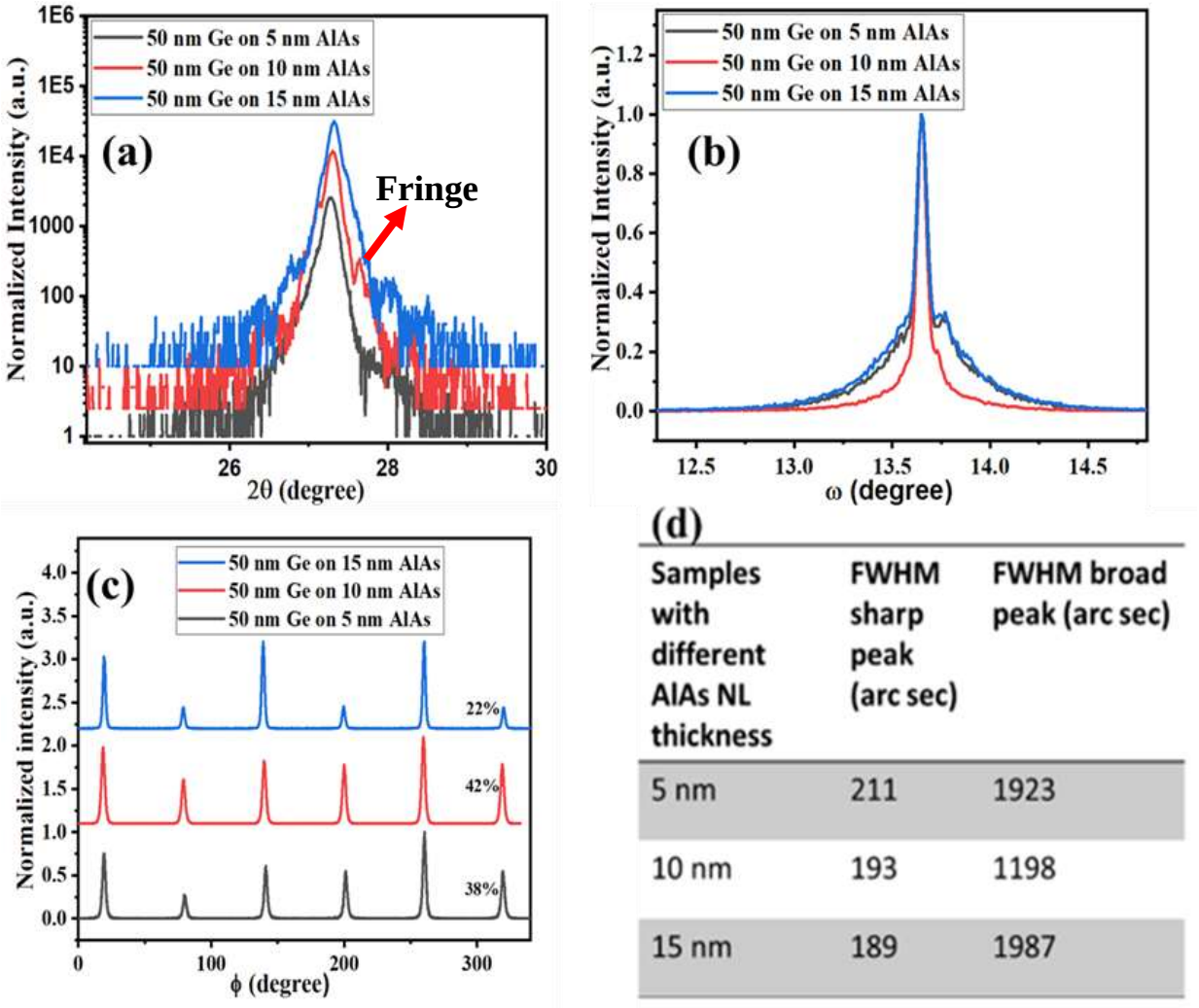

Samples with different AlAs NL thickness	FWHM sharp peak (arc sec)	FWHM broad peak (arc sec)
5 nm	211	1923
10 nm	193	1198
15 nm	189	1987

Figure 8: (a) ω-2θ scan, (b) rocking curve measurement, (c) phi-scan and (d) FWHM value of rocking curve measurement for sample with 5, 10 and 15 nm AlAs NL thicknesses.

Single crystalline Ge (111) is observed for all three samples from the ω-2θ scans (Fig. 8(a)). Prominent fringes for 10 nm AlAs sample indicates better heterointerface between substrate and film and/or flat Ge surface which is also consistent with the AFM results. An estimation of the crystal quality is also done by examining the rocking curve measurement as shown in Fig. 8(b). Here, the FWHM value for sample with AlAs NL thickness of 15 nm is almost the same as compared to the sample with AlAs NL thickness of 5 nm. However, the FWHM value for the sample with AlAs NL thickness of 10 nm relatively improves as compared with the other two samples. Therefore, the use of an AlAs NL of 10 nm growth at 700°C, is an optimum growth window for further investigation on improving Ge thin film crystal quality growth on sapphire. The phi scan (Fig. 8(c)), which gives the qualitative estimation of the crystal quality on a global

scale reveals that the effect of 60° rotational twins is maximum for a sample with 10 nm AlAs NL, although RC shows the best crystal quality for this sample. Twin % calculated from phi-scan only tells us about the volume of twinned material not the density of twin boundary which is responsible for RC broadening [23].

Conclusion:

Ge has been epitaxially grown on c-plane sapphire substrates. High lattice mismatch and interface energy results in 3D growth, high twinning, and multiple crystal orientations in growth direction. Three primary rotational domains are observed at lower growth temperature during direct growth of Ge on sapphire. At higher growth temperatures (600°C and 800°C), three primary rotational domains reduced to two. The result was to find a growth window at 600°C.

With introduction of a thin AlAs NL, the surface and material quality improved which is evident from smoother surface, single epitaxial orientation, sharper RC, and a single domain. The lowest FWHM (213 arcsec) and twining (19.4%) is observed at 700°C with highest surface roughness (32 nm). Further, the effect of varying the AlAs NL thickness on Ge was also investigated. A 10 nm thick NL was found to be the optimum thickness when considering surface roughness and RC line width. The crystal quality was also compared to a reference sample of Ge grown directly on a Ge substrate. This indicated there is still a room for improvement. We are optimistic that further growth optimization using different growth strategies such as a two-step growth method, with annealing, will result in an even high-quality Ge. In addition, investigation of the growth of quality GeSn, SiGe and, SiGeSn on sapphire is also a logical next step.

Acknowledgements:

The authors acknowledge the financial support of the National Aeronautics and Space Administration (NASA) Grant/Contact/Agreement No. 80NSSC19M0145 issued through the Arkansas NASA EPSCoR program. The authors also acknowledge the financial support by the Institute of Nanoscale Science and Engineering, University of Arkansas, and the Project "Quantum Interfaces of Dissimilar Materials funded by National Science Foundation (NSF) (Grant No.1809054).

References

[1] R. Geiger, T. Zabel, and H. Sigg, "Group IV direct band gap photonics: Methods, challenges, and opportunities," *Front. Mater.*, vol. 2, no. 52, July, 2015.

[2] T. Fujii *et al.*, "Development of an epitaxial growth technique using iii-v on a si platform for heterogeneous integration of membrane photonic devices on si," *Appl. Sci.*, vol. 11, no. 4, pp. 1–22, 2021.

[3] H. Ye and J. Yu, "Germanium epitaxy on silicon," *Sci. Technol. Adv. Mater.*, vol. 15, no. 2, 2014.

[4] J. S. Park, M. Tang, S. Chen, and H. Liu, "Heteroepitaxial growth of iii-v semiconductors on silicon," *Crystals*, vol. 10, no. 12, pp. 1–36, 2020.

[5] B. Shi, Q. Li, and K. M. Lau, "Epitaxial growth of high quality InP on Si substrates: The role of InAs/InP quantum dots as effective dislocation filters," *Journal of Applied Physics*, vol. 123, no. 19. 2018.

[6] T. E. Crumbaker, H. Y. Lee, M. J. Hafich, and G. Y. Robinson, "Growth of InP on Si substrates by molecular beam epitaxy," *Applied Physics Letters*, vol. 54, no. 2. pp. 140–142, 1989.

[7] S. Pan *et al.*, "Recent progress in epitaxial growth of III-V quantum-dot lasers on silicon substrate," *Journal of Semiconductors*, vol. 40, no. 10. 2019. https://doi.org/10.3390/ma13102315

[8] A. E. Zhukov *et al.*, "InAs/GaAs quantum dot microlasers formed on silicon using monolithic and hybrid integration methods," *Materials*, vol. 13, no. 10. 2020. https://doi.org/10.3390/ma13102315

[9] T. Soga, S. Hattori, S. Sakai, M. Takeyasu, and M. Umeno, "Characterization of epitaxially grown GaAs on Si substrates with III-V compounds intermediate layers by metalorganic chemical vapor deposition," *J. Appl. Phys.*, vol. 57, no. 10, pp. 4578–4582, 1985.

[10] T. M. Burbaev *et al.*, "Comprehensive study of structural and optical properties of LT-GaAs epitaxial structures," *Bull. Lebedev Phys. Inst.*, vol. 40, no. 8, pp. 219–224, 2013.

[11] M. Yamaguchi, A. Yamamoto, M. Tachikawa, Y. Itoh, and M. Sugo, "Defect reduction effects in GaAs on Si substrates by thermal annealing," *Appl. Phys. Lett.*, vol. 53, no. 23, pp. 2293–2295, 1988.

[12] D. S. Abramkin *et al.*, "Influence of a Low-Temperature GaAs Dislocation Filter on the Perfection of GaAs/Si Layers," *Optoelectron. Instrum. Data Process.*, vol. 54, no. 2, pp. 181–186, 2018.

[13] M. O. Petrushkov *et al.*, "Impact of LT-GaAs layers on crystalline properties of the epitaxial GaAs films grown by MBE on Si substrates," *J. Phys. Conf. Ser.*, vol. 741, no. 1, 2016.

[14] Yu. B. Bolkhovityanov and O. P. chelyakov, "GaAs epitaxy on Si substrate: Modern

status of research an dengineering," *Uspekhi Fiz. Nauk*, vol. 178, no. 5, p. 459, 2008.

[15] M. Yamaguchi, M. Tachikawa, Y. Itoh, M. Sugo, and S. Kondo, "Thermal annealing effects of defect reduction in GaAs on Si substrates," *J. Appl. Phys.*, vol. 68, no. 9, pp. 4518–4522, 1990.

[16] S. K. Saha *et al.*, "GaAs epitaxial growth on R-plane sapphire substrate," *J. Cryst. Growth*, vol. 548, no. August, p. 125848, 2020.

[17] S. K. Saha *et al.*, "Crystalline GaAs Thin Film Growth on a c-Plane Sapphire Substrate," *Cryst. Growth Des.*, vol. 19, no. 9, pp. 5088–5096, 2019.

[18] T. P. Humphreys *et al.*, "Heteroepitaxial growth and characterization of GaAs on silicon-on- sapphire and sapphire substrates," *Appl. Phys. Lett.*, vol. 54, no. 17, pp. 1687–1689, Apr. 1989.

[19] R. Kumar *et al.*, "GaAs Layer on c-plane Sapphire for Light Emitting Sources," *Appl. Surf. Sci.*, p. 148554, 2020.

[20] D. J. Godbey and M. E. Twigg, "The nucleation and growth of germanium on (1102) sapphire deposited by molecular-beam epitaxy," *Journal of applied physics*, 1991. https://doi.org/10.1063/1.348392

[21] D. J. Godbey *et al*, "Single-crystal germanium grown on (1102) sapphire by molecular beam epitaxy," *Journal of applied physics*, 1989. https://doi.org/10.1063/1.101068

[22] Z. Lu, X. Wen, M. A. Washington, and T. M. Lu, "Heteroepitaxy of High-Mobility Germanium on Sapphire (0001) with Magnetron Sputtering," *ACS Applied Electronic Materials*, vol. 2, no. 6. pp. 1635–1644, 2020.

[23] D. Pelati *et al.*, "GaAs (1 1 1)epilayers grown by MBE on Ge (1 1 1): Twin reduction and polarity," *J. Cryst. Growth*, vol. 519, no. May, pp. 84–90, 2019.